

## Influence of hydrogen bonding interactions on the properties of ultraviolet-curable coatings

Lu Shen,<sup>1,2</sup> Jian Zheng,<sup>1,2</sup> Ying Wang,<sup>1,2</sup> Mangeng Lu,<sup>1</sup> Kun Wu<sup>1</sup>

<sup>1</sup>Key Laboratory of Cellulose and Lignocellulosics Chemistry, Guangzhou Institute of Chemistry, Chinese Academy of Sciences, Guangzhou, People's Republic of China

<sup>2</sup>University of Chinese Academy of Sciences, Beijing, People's Republic of China

Correspondence to: K. Wu (E-mail: wukun@gic.ac.cn)

**ABSTRACT:** Phenolic novolac type epoxy resin has been modified with acrylic acid (AA) and 2-acrylamido-2-methyl-1-propanesulfonic acid (AMPS) to form ultraviolet-curable coatings, and integrated performances of the coatings were evaluated. It was found that the hydrogen bonding interactions among the oligomers became stronger along with the increase of AMPS content, thus the oligomer viscosity and a variety of polymer properties were affected. The polar hydrogen bond donors significantly enhanced the adhesion strength and surface wetting behavior of the coatings. Meanwhile, hydrogen bonding interactions can also reinforce the three-dimensional structure of the film as in polymeric state, which potentially increased its glass transition temperature and mechanical properties. Results of chemical resistance showed that coatings modified with moderate amount of AMPS could be completely removed in several minutes when exposed to alkali solution or anhydrous ethanol. With these attractive features, modified films had prospective applications in temporary protective coatings. © 2015 Wiley Periodicals, Inc. *J. Appl. Polym. Sci.* **2016**, *133*, 43113.

**KEYWORDS:** coatings; cross-linking; hydrophilic polymers; photopolymerization

Received 9 September 2015; accepted 2 November 2015

DOI: 10.1002/app.43113

### INTRODUCTION

Photopolymerization science and technology has attracted a significant amount of attention due to its various industrial applications. Among various methods of photo-curing, the ultraviolet (UV) curing process is becoming of increasing importance in different fields, such as protective coatings, electronics, adhesives, and inks. This rapid growth of the UV curing technique is attributed to the significant advantages of lower energy consumption, less environmental pollution, lower process costs, excellent film quality, and high efficiency in production.<sup>1–3</sup>

Epoxy acrylate (EA) resins, which introduce vinyl ester groups with carbon–carbon double bonds at the end of the epoxy resin, have been widely used as UV-curing oligomers in many industries for their excellent adhesive and non-yellowing properties, hardness, and chemical resistance.<sup>3–5</sup> However, apart from having several outstanding characteristics of cured films, the use of EA resins is limited because of its weak mechanical properties. The inherent brittleness shows poor fracture toughness, poor resistance to crack propagation, and low impact strength of the cured films, which has limited their applications in the field of composites and coatings.<sup>2,6,7</sup>

Temporary protective coatings are widely used to reduce the susceptibility of substrates, for instance, glass substrates have one or more functional coatings to avoid mechanical damage during processing, handling, shipping, or storage. And the removal of the coatings greatly simplifies cleaning procedure of the surface, whereby surface contamination is eliminated by peeling or washing off the outer membrane.<sup>8–10</sup>

It has been reported that hydrogen bonding affects a variety of monomer and polymer properties. Viscosity, surface wetting behavior, glass transition temperatures, and mechanical properties associated with the polymers would be significantly influenced by these relatively strong, noncovalent interactions (generally 3–6 kcal/mol). This is surely because the hydrogen bonding interactions play an important role in monomer configuration and mobility on the molecular level, which in turn dramatically impact monomer and polymer properties through summation effects.<sup>11–13</sup>

In the recent years, 2-acrylamido-2-methyl-1-propanesulfonic acid (AMPS) has been reported in the hydrogels synthesis. It received great attention due to its strongly ionizable sulfonate group which has better hydrophilic properties than the carboxyl group. This can be reflected by the fact that AMPS dissociate completely in the overall pH range.<sup>14–16</sup> Besides, the acrylic

**Table I.** Molar Ratio of the Reactive Monomer

Sample	Epoxy group	Molar ratio	
		AMPS	AA
NEA-1	1	0	0.9
NEA-2	1	0.9 × 5%	0.9 × 95%
NEA-3	1	0.9 × 10%	0.9 × 90%
NEA-4	1	0.9 × 20%	0.9 × 80%

double bond of AMPS can participate in free-radical polymerization. Therefore it could be activated under UV light and connect with acrylic acid (AA) to form a network through photochemical reactions.<sup>17–19</sup> However, few reports have been found about using AMPS as a modifier material to improve the hydrophilic of UV-curable coatings, which would alter the strength of hydrogen bonding and a range of coating properties ultimately.

In this work, a series of UV-curable hydrophilic resins based on phenolic novolac type epoxy resin were synthesized by mixing AMPS and AA in different ratios to participate in the epoxy ring opening reaction jointly. The strength of hydrogen bonding interaction generally increased along with more polar groups introduced. It should be very valuable to investigate the influence of hydrogen bonding systematically. Consequently, integrated properties of the photocured coatings were investigated by regulating monomer ratio to alter the hydrogen bonding strength.

## EXPERIMENTAL

### Materials

Acrylic acid (AA, 99%), 2-acrylamido-2-methyl-1-propanesulfonic acid (AMPS, 98%), hydroquinone (HQ, 99%), triphenylphosphine (TPP, 99%) were all purchased from Aladdin, China. Phenolic novolac type epoxy resins (NPPN-631, 0.56–0.60 epoxy value) was provided by Nan Ya Plastics Corporation, Taiwan. Trimethylol propane triacrylate (TMPTA) was supplied by Huizhou Kesheng Trading Co. Darocur<sup>®</sup> 1173 (2-hydroxy-2-methyl-1-phenyl-1-propanone, BASF, Germany) was used as free-radical photoinitiator. Glass slides were provided from Guangzhou Xindi Experimental Equipment Co. and they were used as substrates for all coating applications. All other reagents were used as received without further purification.

### Synthesis of AMPS-Modified Epoxy Resin

30 g novolac epoxy resins (NE) and 0.15 g HQ (inhibitor) were added into a 150-mL three-necked glass flask equipped with stirrer and nitrogen inlet. Then, the reaction system was stirred and heated to 80°C. As listed in Table I, the mixture of AMPS, AA in varying molar ratios, and 0.3 g TPP (catalyst) were dropwise added through the side neck of the flask over a period of 1 h. The reaction was carried out for about 4 h to obtain the modified novolac epoxy resins (NEA).

The AMPS powder was dissolved in water (mass ratio 1:1) before being dropped into the epoxy system to get a homogeneous reaction. After reaction, the water was eliminated from the

obtained resin by rotary evaporation. The synthesis pathway is given in Scheme 1.

### Test Specimen Preparation

A certain amount of the above prepared NEA resins, 3 wt % photoinitiator Darocur 1173, in combination with 10 wt % TMPTA as reactive diluent were weighted. And then the mixture was stirred intensively at 60°C for several minutes until the hybrid system was homogeneous. Meanwhile, the glass substrates were rinsed with acetone and ethanol, and dried with lens cleaning paper. After that, a small amount of mixture was coated onto glass substrates at room temperature.

The coated film samples were placed under a medium-pressure mercury lamp with power of 1000 W (LT-UV102, Blue sky special lamp Co., Hebei, China) in the atmosphere of air. A UV radiation dose of about 500 mJ/cm<sup>2</sup> was applied to the samples at room temperature (25°C) and the main peak absorption wave length was 365 nm.

After UV curing procedure, the thickness of the coatings was determined with a digital display micrometer (Precision Instrument Co., Shanghai, China), and it ranged from 20 to 30 μm. The glass panels used were subjected to different performance tests.

Furthermore, the strip-shaped specimens (80 mm × 10 mm × 1 mm) were prepared in a Teflon<sup>™</sup> mold which was used to obtain a smooth surface. After about 2 min of irradiation, the samples were acquired for mechanical properties tests.

### Characterization

**FT-IR Spectra.** Fourier transform infrared (FT-IR) spectra were recorded on a Nicolet 5100 spectrometer in the region of 400–4000 cm<sup>-1</sup>.

**<sup>1</sup>H NMR Spectra.** Nuclear magnetic resonance (NMR) spectra were obtained on a Bruker DRX-400 spectrometer. Deuterated dimethyl sulfoxide (DMSO-d<sub>6</sub>) was used as the solvent.

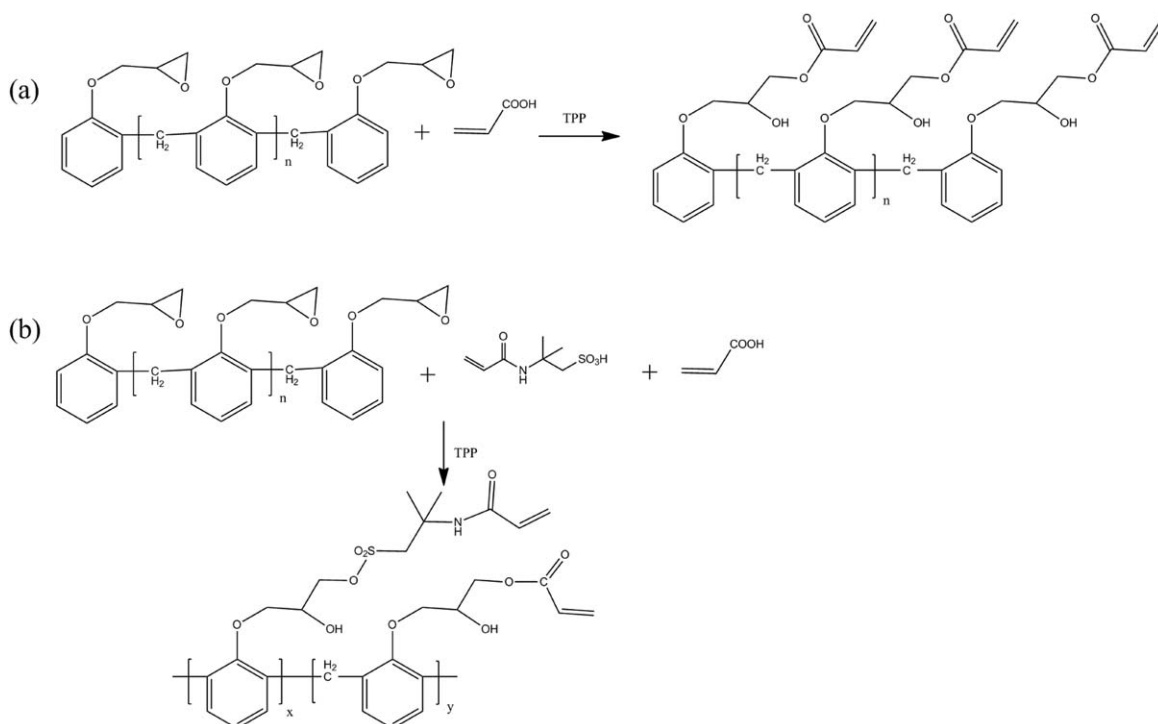
**Gel Content.** Gel content of the films was determined by measuring the weight loss after 72 h extraction with acetone at 25°C. The gel content was calculated as  $m_2/m_1 \times 100$ , where  $m_2$  is the weight of the insoluble residue after extraction and  $m_1$  is the initial weight of the dried film.

**Tape Adhesion.** Tape adhesion was measured in accordance with the corresponding standard test methods as ASTM D-3359.

**Hardness.** Pencil hardness test was applied on coated glass plates, and it was measured according to ASTM D-3363. Shore A hardness of the films was determined by ASTM D 2240.

**Chemical and Water Resistance.** Chemical and water resistance of the UV-cured films was determined by immersing coated film samples into various chemicals at 25°C. The coatings were examined after a certain time. Visual comparisons were made with untreated panels and rated in three categories.

**Contact Angle Measurements.** Surface static contact angles were measured with 2 μL of distilled water droplet placed on the cured film by JC-2000D (Shanghai zhongchen digital



**Scheme 1.** Synthesis routes for the resins (a) NEA-1: novolac epoxy acrylate resin and (b) NEA-2,3,4: novolac epoxy sulfonic acid resin.

technology equipment Co., China). The test results were the average of five samples.

**Water Swelling Ratio of the Cured Films.** It was measured by the method as follows: a pre-weighed dry specimen (about 0.5 g) was immersed in deionized water at 35°C. Then the film was taken out and free water on the surface was absorbed by filter paper. The weight of sample was monitored at regular time interval (12 h) to a constant weight. The water swelling ratio (SR) was calculated as follows:  $SR = (W_s - W_d)/W_d \times 100$ , where  $W_s$  is the weight of swollen sample and  $W_d$  is the weight of dry sample.<sup>14</sup>

**Mechanical Properties.** Mechanical properties of the UV-cured strip-shaped specimens were determined by standard tensile stress-strain and impact resistance tests. Standard tensile stress-strain experiments were performed at room temperature on a Materials Testing Machine RGM-3030, using a cross-head speed of 5 mm/min. Besides, the unnotched impact strengths were tested according to the Chinese Standard GB/T1043-1993 using a Charpy Impact Machine Tester (WPM, China). The surface of strip samples was polished smooth by sandpaper before tests, and reported data is the average of five measurements.

**Scanning Electron Microscope.** The morphology of the impact fracture surface was observed by a Philips XL30 scanning electron microscope (SEM). The crack section was measured after metal spraying process and the accelerating voltage is 15 kV.

**Differential Scanning Calorimeter.** The glass transition temperature of the samples was tested by differential scanning calorimeter (DSC, TA Q200, USA). All of the cured samples (about 10 mg) were heated from -20°C to 150°C under a nitrogen

atmosphere at the flow of 20 mL/min. Besides, the thermograms were recorded at a heating rate of 20°C/min.

**Thermogravimetry Analysis.** The thermal stability of samples was characterized by a thermogravimetric analyzer (TGA, Pyris-1, Perkin-Elmer, USA). About 5 mg of the curing powder were introduced into the thermobalance, and then heated from 35 to 800°C at a heating rate of 10°C/min and in nitrogen flow of 20 mL/min, respectively.

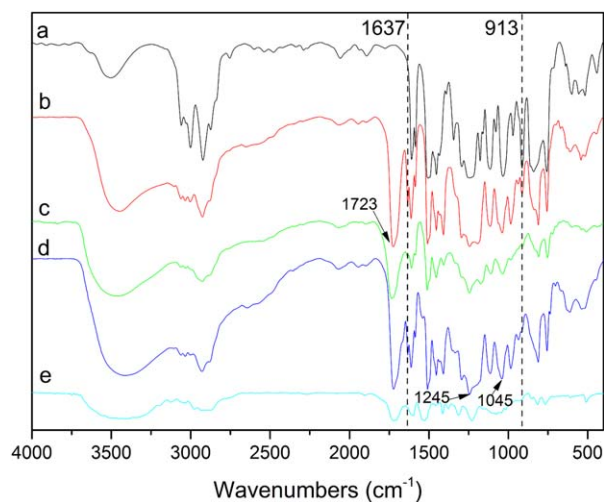


**Figure 1.** FT-IR spectra of (a) NE: novolac epoxy resin; (b) NEA-1; (c) CNEA-1: cured NEA-1 resin; (d) NEA-3; and (e) CNEA-3: cured NEA-3 resin. [Color figure can be viewed in the online issue, which is available at [wileyonlinelibrary.com](http://wileyonlinelibrary.com).]

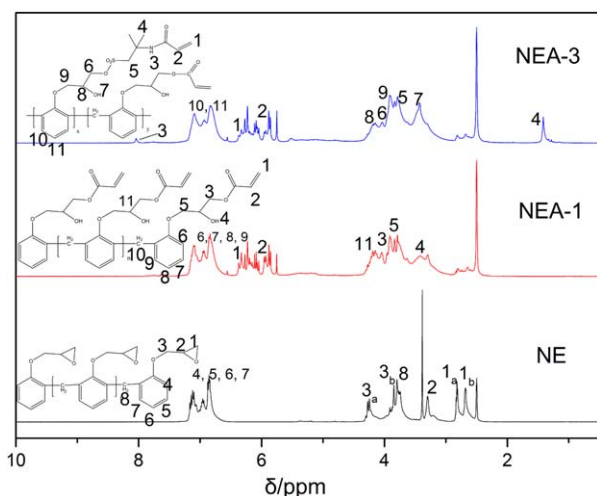


**Figure 2.**  $^1\text{H}$  NMR (DMSO- $d_6$ ) spectra of (a) NE; (b) NEA-1; and (c) NEA-3. [Color figure can be viewed in the online issue, which is available at [wileyonlinelibrary.com](http://wileyonlinelibrary.com).]

## RESULTS AND DISCUSSION

### FT-IR Spectra Analysis

Figure 1 shows the FT-IR spectra of NE, NEA-1, and NEA-3 resins. For NEA-1 resin, the characteristic broad band at  $3442\text{ cm}^{-1}$  for hydroxyls and band at  $1723\text{ cm}^{-1}$  for carbonyl group were observed, respectively. Meanwhile, the intrinsic absorption of epoxy group at  $913\text{ cm}^{-1}$  disappeared, suggesting that the chemical reaction between epoxy and acrylic acid occurred as expected [Scheme 1(a)]. In Figure 1(d), the characteristic absorption peaks of AMPS were shown at  $1045\text{ cm}^{-1}$  due to S=O group. Besides, the absorption peaks appeared at around  $1294\text{--}1173\text{ cm}^{-1}$ ,  $1245\text{ cm}^{-1}$  were assigned to the alkyl ether linkages formed by the reaction between NE and AMPS, AA.<sup>1,14,20</sup>

The cured films were also characterized by FT-IR, as presented in Figure 1(c,e). It could be clearly seen that the absorption of  $\text{—CH=CH}_2$  at  $1637$  and  $981\text{ cm}^{-1}$  disappeared after UV irradiation, as well as the absorption at  $810\text{ cm}^{-1}$  attributed to  $\text{=C—H}$ . This confirmed that NEA coatings have been completely cured.

### $^1\text{H}$ NMR Analysis

In case of  $^1\text{H}$  NMR spectra of NEA (Figure 2), characteristic peaks of  $\text{—CH=CH}_2$  formed at  $\delta = 5.93\text{--}6.37\text{ ppm}$  supported the formation of NEA-1 and NEA-3 via the chemical reaction between NE and acid groups. The characteristic peaks presented at  $8.0\text{ ppm}$  and  $1.4\text{ ppm}$  were ascribed to the amide ( $\text{—NH—C=O}$ ) and methyl ( $\text{—CH}_3$ ) protons of NEA-3, respectively. Furthermore, the peaks of epoxy group protons almost disappeared at  $\delta = 2.67\text{--}2.83\text{ ppm}$ , which also confirmed the reaction.

### Viscosity

Viscosity is an important property of oligomers that controls the diffusion process in photopolymerization reactions.<sup>21</sup> Figure 3 shows the viscosity of NEA resins at  $60^\circ\text{C}$ . According to the experimental data, the viscosity of the oligomer was greatly improved as the increased AMPS content. The viscosity

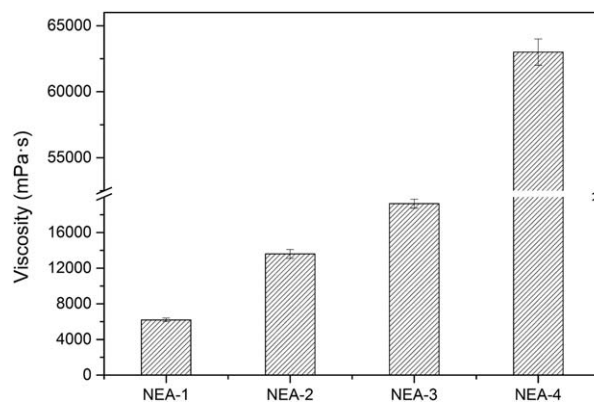


**Figure 3.** The viscosity of NEA resins at  $60^\circ\text{C}$ .

transformation may contribute to the increased molecular weight of modified resins, as materials with higher molar masses usually have higher viscosities.<sup>22</sup> Since NEA resins are synthesized by end-capping NEA with AMPS and AA in different ratios, the molar mass of AMPS ( $207.24$ ) is about three times greater than that of AA ( $72.06$ ). Accordingly, the molecular weight of the resins increases as more AMPS is added.

Besides, the intermolecular and intramolecular hydrogen bonds formed among NEA molecules is another important factor that influences the viscosity.<sup>23</sup> NEA oligomer has a large amount of hydroxyl and carbonyl groups, the incorporation of more hydrogen bonded sulfonate groups from AMPS would lead to higher interactions between molecules which hindered the movement of chain segment, resulting in the increased viscosity.<sup>24</sup> It was supported by the FT-IR spectra shown in Figure 4.

Hydrogen bonding interactions are often examined through analyzing the carbonyl stretching absorption.<sup>25</sup> It was observed that the peak attributing to the hydrogen bonded carbonyl (about  $1703\text{ cm}^{-1}$ ) is smaller than that assigning to the nonhydrogen bonded carbonyl (about  $1723\text{ cm}^{-1}$ ) in all systems. However, the peak intensity of the hydrogen bonded carbonyl

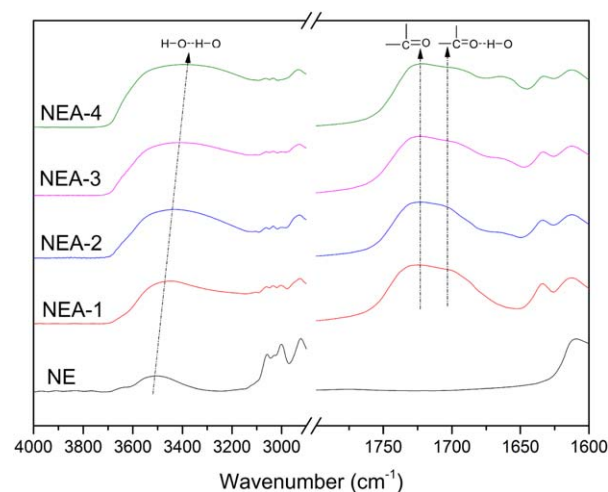


**Figure 4.** FT-IR spectra of the OH stretching region and carbonyl stretching region for NEA resins. [Color figure can be viewed in the online issue, which is available at [wileyonlinelibrary.com](http://wileyonlinelibrary.com).]

**Table II.** Physical Characterizations and Chemical Resistance of Cured Films on Slides

Sample	Gel content (%)	Tape adhesion loss (%)	Pencil hardness (H, on glass)	Chemical resistance test				
				Shore A hardness	NaOH (2% wt, 24 h)	HCl (2% wt, 36 h)	Anhydrous ethanol (12 h)	Deionized water (36 h)
NEA-1	92.97	0B	5	82	a	a	a	a
NEA-2	89.73	1B	5	80	c	a	a	a
NEA-3	84.80	2B	5	80	c	a	b	a
NEA-4	79.53	4B	4	78	c	a	b	a

a, unaffected; b, loss in gloss and adhesion; c, loss in gloss, adhesion, and weight.

barely changed, even though the content of amide group ( $O=C-NH$ ) from AMPS in NEA system became larger. The content of AMPS in NEA system did not affect carbonyl hydrogen bonds between modified molecules obviously. It may be attributed to the equivalent content of carbonyl group in AMPS and AA. Besides, the structure of the modified resins was similar.

Nevertheless, the OH stretching peak of NEA system shifted toward lower frequencies as the incorporation of more AMPS, providing the evidence of the formation of stronger intermolecular hydrogen bonding between NEA oligomers. It could be inferred that the intermolecular  $OH...OH$  hydrogen bonds is the major factor that strengthen the interactions between NEA molecules.<sup>19</sup>

Moreover, hydrogen bonding is generally sensitive to the temperature. Strong hydrogen bonding through the secondary hydroxyls is reported to be the main cause of the high viscosity of EA resins.<sup>26</sup> The viscosity of NEA oligomers at 25°C were over 1,00,000 cps, which decreased steeply as the temperature increased up to 60°C. This tremendous change in viscosity can be ascribed to the fact that the strength of the hydrogen bonds tends to decrease at a higher temperature.<sup>11</sup>

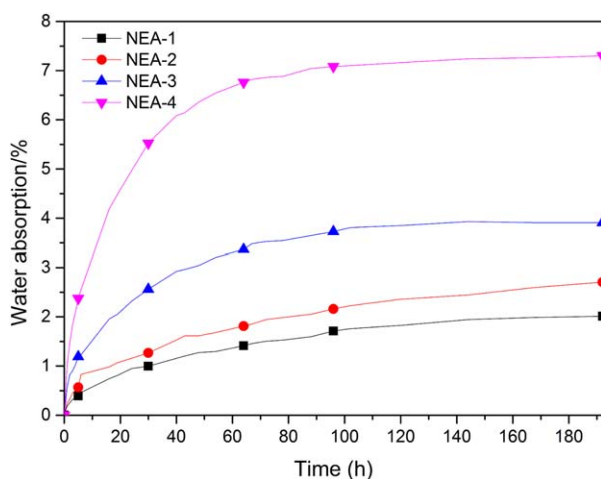
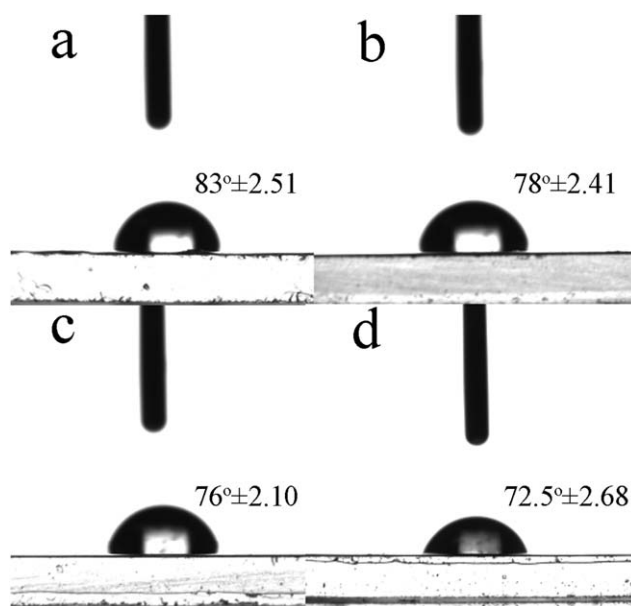


**Figure 5.** Water swelling ratio of the films change with time. [Color figure can be viewed in the online issue, which is available at wileyonlinelibrary.com.]

### Physico-Chemical Properties of UV Curable Coatings

The values for various physico-chemical properties of NEA coatings were summarized in Table II. The gel fraction was measured to confirm the cross-linking degree of the films after UV curing.<sup>27</sup> Since a tightly cross-linked polymeric network would obtain a high gel content value. Apparently, the introduction of AMPS would decrease the cross-link density of films.

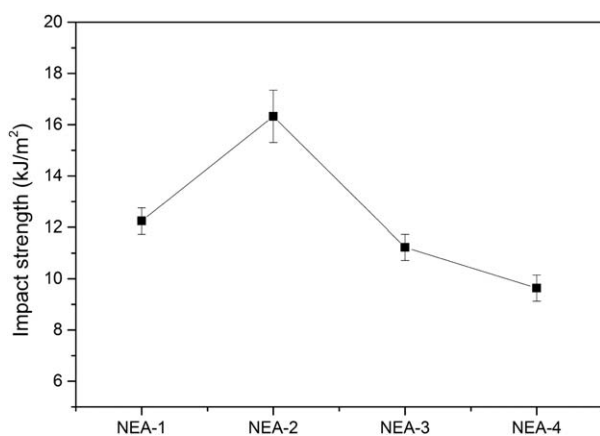
In general, the cured EA coatings had bad adhesion on glass, even the alkoxy silane-modified EA had 70% tape adhesion loss.<sup>28,29</sup> The introduction of AMPS was propitious to improve the adhesion between films and the substrates greatly. This is surely due to the strong hydrogen bonding formed between amide sulfonate groups from AMPS and the polar surface of glass substrates.<sup>30</sup> When the percentage of AMPS in the oligomer increased, the pencil hardness of the coatings decreased from 5H to 4H. The Shore A hardness showed the same trend. The reduced hardness may be attributed to the lower content of rigid benzene rings in NEA-4 oligomer compared with NEA-1.<sup>31</sup>



**Figure 6.** Contact angle images of (a) NEA-1; (b) NEA-2; (c) NEA-3, and (d) NEA-4 coatings.

**Table III.** Strain–Stress Analysis

Sample	Tensile strength (MPa)	Elongation at break (%)	Modulus (MPa)
NEA-1	27.45	11.44	380
NEA-2	27.33	13.20	350
NEA-3	28.62	18.46	320
NEA-4	38.66	20.48	300

**Figure 7.** The impact strengths of cured films.

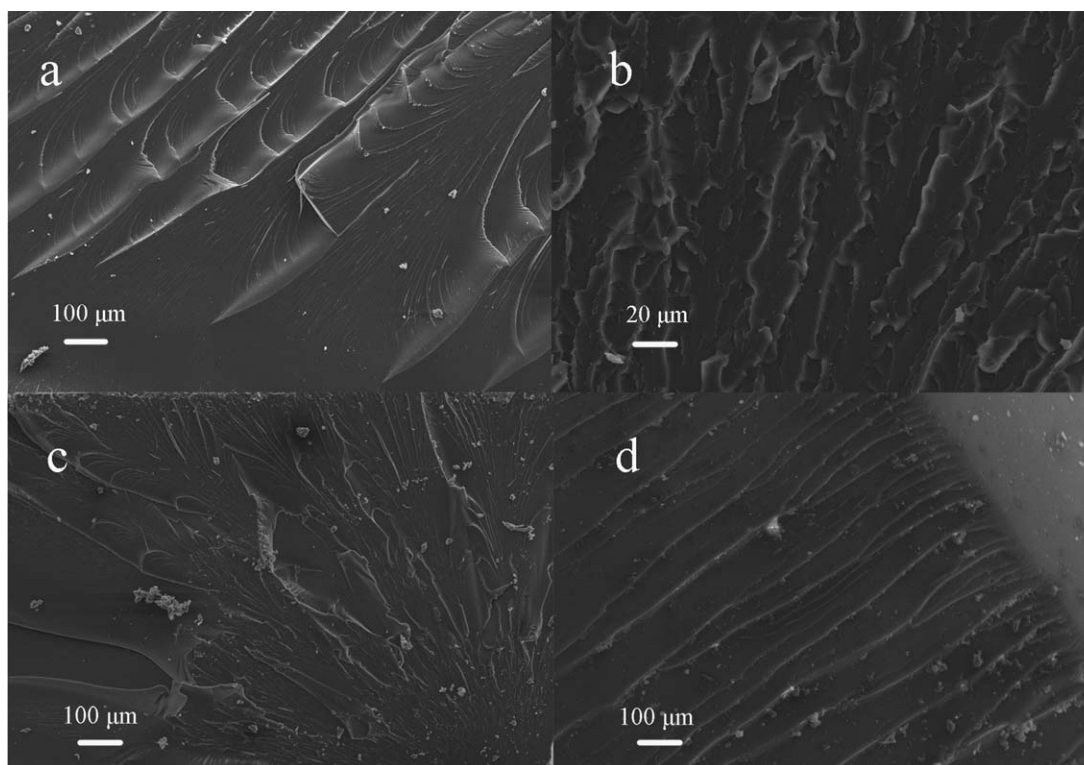
To test the chemical resistance, cured films were immersed in anhydrous ethanol, 2 wt % HCl and 2 wt % NaOH respectively, at room temperature. EA films have good solvent and chemical

resistance performance, they could resist the attack of 5 wt % acid and alkali in 5 days.<sup>1</sup> However, the experimental results showed that the solvent and chemical resistance of the modified films had been weakened with the increasing AMPS content. When exposed to alkali solution, the NEA-4 coatings collapsed in less than 3 min and were completely removed from the substrate in 6 min. In addition, it could be wiped off from the substrate by soaking in anhydrous ethanol for 3 min as well. However, the NEA-4 films were found to be unaffected after 24 h in acid and 36 h in deionized water, respectively. This is mainly because the incorporation of more strongly ionizable sulfonate groups enables modified films with pH-independent swelling behavior.<sup>15,16</sup> What's more, polar solvent would weaken hydrogen bonding interactions formed between the polymer and the silanol groups present at the glass surface, resulting in a partial or total loss of adhesion.

From the above results, it proved that films with moderate amount of AMPS added had a potential use in temporary protective coatings. The films could resist acid and preserve the status quo in a mild environment, while being wiped off from the glass substrate by soaking in alkali solution or polar solvent easily.

#### Hydrophilicity of the Coatings

The alterations of water SR change with time are clearly depicted in Figure 5. The water absorption values of NEA-1, NEA-2, NEA-3, and NEA-4 after 192 h were 2.01%, 2.71%, 3.91%, and 7.30%, respectively. The massive increase was partly due to the reduced cross-linking density of AMPS-modified structure, which allowed more water to reside between the

**Figure 8.** SEM images of various fracture morphologies after impact tests (a) NEA-1; (b) NEA-2; (c) NEA-3; and (d) NEA-4.

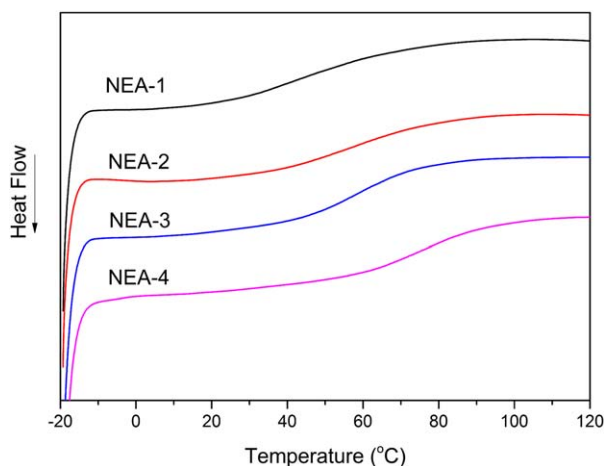


**Figure 9.** DSC curves of UV-cured NEA films. [Color figure can be viewed in the online issue, which is available at [wileyonlinelibrary.com](http://wileyonlinelibrary.com).]

polymer chains.<sup>20</sup> Because dense network would not only hinder the chain mobility, but also reduce the space to retain water, and eventually restrict the water uptake values. Besides, the hydrophilic nature of sulfonate groups was another important reason for the improved water absorbing capacity.<sup>32</sup> In Figure 6, the average contact angle values were shown with the standard deviation. With more AMPS content, a decreased contact angle was observed. Strong hydrophilic ability of sulfonate groups increased the hydrogen bonding interaction between polymer chains and water molecules, thus resulting in a better wettability and a lowered contact angle values.<sup>33,34</sup>

#### Mechanical Properties

Evaluated stress–strain data of strip-shaped specimens are listed in Table III. Test specimens of NEA series were broken without yield, it revealed that the specimens were hard and brittle. The tensile strength and elongation at break of the films increased along with more AMPS loading, whereas the Young's Modulus decreased progressively. The improved tensile strength demonstrated that hydrogen bonding interactions would serve to reinforce the mechanical properties of cross-linked polymer.<sup>11</sup> The reduced modulus was mainly due to the reduction in cross-linking density of cured film, which was a cause of lowered hardness as well.<sup>35</sup>

The impact resistance is usually used to evaluate the toughness of a material which reflects the ability to absorb the energy of a rapidly applied load.<sup>36</sup> Figure 7 shows the dependence of the impact strength on the content of AMPS in cured NEA resins, it was observed that NEA-2 had the maximum impact strength.

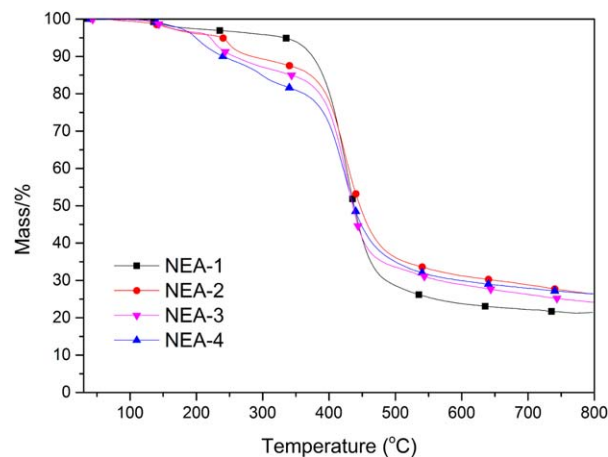


**Figure 10.** Thermogravimetric analysis of cured films. [Color figure can be viewed in the online issue, which is available at [wileyonlinelibrary.com](http://wileyonlinelibrary.com).]

Two major factors may compete with each other to influence the impact resistance of the cross-linked networks. Firstly, with more polar sulfonate groups introduced into the cured network, the stronger hydrogen bond would block the molecular chains rotate, and thus the films absorbed less energy under external force. Contrary to this, a lower cross-linking density increased the chain mobility by reducing links between the polymeric backbones.<sup>19</sup> Each of the two factors was related to the content of AMPS, resulting in the fact that impact resistance of the films were closely dependent on the monomer molar ratio. Consequently, there was a suitable range in the content of AMPS to get improved integrated properties.

The fractured surface morphology has been investigated by SEM (Figure 8). It depicted that the cured NEA networks exhibited smooth and homogeneous morphology surface, representing a homogeneous material. A smooth fracture surface indicates a brittle behavior, corresponding to poor resistance to impact stresses.<sup>37</sup> While a combination of shear cusps and coarse features emerged on the fracture surface of NEA-2 films, which corresponded with its better impact resistance.

#### Thermal Performance Analysis

Glass transition temperatures ( $T_g$ ) of the UV-cured films were investigated by DSC. Figure 9 shows the DSC curves of NEA and the  $T_g$  values are reported in Table IV. It was observed that the introduction of AMPS would increase the  $T_g$  values. This could be ascribed to the enhanced interaction among various chain segments. Although cross-linking degree of modified films

**Table IV.**  $T_g$  and Thermal Stability Data of the Cured Films

Sample	$T_g$ (°C)	Weight loss % at 100°C	5 wt % loss temperature (°C)	10 wt % loss temperature (°C)	50 wt % loss temperature (°C)	Char yield (wt %, 800°C)
NEA-1	43.62	0.01	335.4	375.4	437.9	21.43
NEA-2	58.10	0.58	240.4	285.4	447.9	26.37
NEA-3	59.53	0.04	221.1	258.6	436.1	24.16
NEA-4	64.71	0.17	200.2	242.7	437.7	26.47

was lower, the extremely strong interaction of hydrogen bonding was the dominant factor in this case. It blocked the chain movement and reinforced the three-dimensional structure, which could apparently provide enhanced glass transition.<sup>38</sup>

Thermal stability is another important factor for the properties of the UV-cured films, and the thermo-gravimetric analysis (TGA) thermograms of the cured polymers in N<sub>2</sub> are shown in Figure 10. It could be seen that the degradation of the cured resins had three stages: the first decomposition temperature occurred at about 250°C was assigned to the thermal decomposition of unstable sulfonate groups. The second thermal degradation that took place at about 420°C was ascribed to main-chain degradation of polymer. Moreover, the third step observed above 550°C was attributed to the further decomposition of the samples.<sup>39</sup>

In contrast with NEA-1 films, the 5% degradation temperatures ( $T_{d,5\%}$ ) of NEA-4 films decreased from 335.4°C to 200.2°C and the 10% degradation temperatures ( $T_{d,10\%}$ ) decreased from 375.4°C to 242.7°C, respectively. This was attributed to the poor thermal stability of sulfonate groups and the reduced cross-link density of cured modified resins. 50 wt % loss temperature for all the cured films is very close, it may be due to the similar main structure of the modified oligomers. However, the materials with more AMPS content showed a higher char content at 800°C. During the thermal degradation, some interactions may occur between the degradation products of sulfonate groups and aromatic species, which contributed to the formation of sulfone-containing polymer with excellent thermal stability.<sup>40–42</sup>

## CONCLUSIONS

Hydrophilic UV-curing EA coatings modified by AMPS were successfully synthesized. Regular transformation of several polymer properties could be ascribed to the gradually enhanced hydrogen bonding as the incorporation of more polar groups. It was found that hydrogen bonding can favorably affect monomer viscosity, polymer performance, and mechanical properties, even in materials that form highly cross-linked polymeric networks. AMPS-modified resins had a stronger hydrogen bonding interactions deriving from polar groups, it resulted in the higher oligomer viscosity and the improved film adhesion. Contact angles and water absorption measurements demonstrated that hydrophilic surfaces were obtained with incorporation of the amide and sulfonate segments. Results from mechanical characterizations clearly indicated that hydrogen bonding interactions had a significant impact on the fracture strength of the specimens. The tensile strength and elongation at break of NEA series increased with growing AMPS content, but the modulus value went down. Moreover, with stronger hydrogen bonding in the skeleton, the modified cured films exhibited higher glass transition temperature.

## ACKNOWLEDGMENTS

The financial supports from Guangdong Natural Science Foundation, China (No. 2015A030313798), Zhujiang Science & Technology New-star Program of Guangzhou, China (No. 2013J2200016),

and Guangdong Special Support Program-Youth Top-notch Talent (No. 201427032) are acknowledged.

## REFERENCES

1. Bajpai, M.; Shukla, V.; Kumar, A. *Progr. Org. Coat.* **2002**, *44*, 271.
2. Gao, L. P.; Wang, D. Y.; Wang, Y. Z.; Wang, J. S.; Yang, B. *Polym. Degrad. Stab.* **2008**, *93*, 1308.
3. Chattopadhyay, D. K.; Panda, S. S.; Raju, K. *Progr. Org. Coat.* **2005**, *54*, 10.
4. Radhakrishnan, S.; Pethrick, R. A. *J. Appl. Polym. Sci.* **1994**, *51*, 863.
5. Deng, C. L.; Deng, C.; Zhao, J.; Fang, W. H.; Lin, L.; Wang, Y. Z. *Polym. Adv. Technol.* **2014**, *25*, 861.
6. Levchik, S. V.; Weil, E. D. *Polym. Int.* **2004**, *53*, 1901.
7. Xu, K.; Chen, M. C.; Zhang, K.; Hu, J. W. *Polymer* **2004**, *45*, 1133.
8. Lewandowski, K.; Krepski, L. R.; Mickus, D. E. *J. Appl. Polym. Sci.* **2004**, *91*, 1443.
9. Chang, S.; Yang, J. H.; Chien, J. H.; Lee, Y. D. *J. Polym. Res.* **2013**, *20*, 1.
10. O'shaughnessy, R. D.; Krisko, A. J.; Hartig, K. Hydrophilic Surfaces Carrying Temporary Protective Covers, U.S. Pat. 6,902,813 B2 (2005).
11. Lemon, M. T.; Jones, M. S.; Stansbury, J. W. *J. Biomed. Mater. Res. Part A* **2007**, *83A*, 734.
12. Beuermann, S. *Macromolecules* **2004**, *37*, 1037.
13. Lefebvre, D. R.; Elliker, P. R.; Takahashi, K. M.; Raju, V. R.; Kaplan, M. L. *J. Adhes. Sci. Technol.* **2000**, *14*, 925.
14. Atta, A. M.; Ismail, H. S.; Mohamed, H. M.; Mohamed, Z. M. *J. Appl. Polym. Sci.* **2011**, *122*, 999.
15. Gad, Y. H. *Radiat. Phys. Chem.* **2008**, *77*, 1101.
16. Limparyoon, N.; Seetapan, N.; Kiatkamjornwong, S. *Polym. Degrad. Stab.* **2011**, *96*, 1054.
17. Shi, S.; Guo, F.; Xia, Y.; Su, Z.; Chen, X.; Wei, M. *J. Appl. Polym. Sci.* **2011**, *121*, 1661.
18. Nowers, J. R.; Narasimhan, B. *Polymer* **2006**, *47*, 1108.
19. Liu, P.; Gu, A.; Liang, G.; Guan, Q.; Yuan, L. *Progr. Org. Coat.* **2012**, *74*, 142.
20. Zhong, S.; Cui, X.; Cai, H.; Fu, T.; Shao, K.; Na, H. *J. Power Sources* **2007**, *168*, 154.
21. Reghunathan, H. *Adv. Polym. Technol.* **2014**, *33*, 3.
22. Wang, S.; Zou, Y. *J. Appl. Polym. Sci.* **2013**, *129*, 3325.
23. Khatri, C. A.; Stansbury, J. W.; Schultheisz, C. R.; Antonucci, J. M. *Dent. Mater.* **2003**, *19*, 584.
24. Rengasamy, S.; Mannari, V. *Progr. Org. Coat.* **2013**, *76*, 78.
25. Li, D.; Brisson, J. *Polymer* **1998**, *39*, 793.
26. Oprea, S.; Vlad, S.; Stanciu, A.; Macoveanu, M. *Eur. Polym. J.* **2000**, *36*, 373.
27. Wang, X.; Wang, B.; Xing, W.; Tang, G.; Zhan, J.; Yang, W.; Song, L.; Hu, Y. *Progr. Org. Coat.* **2014**, *77*, 94.
28. Li, C.; Cheng, J.; Yang, F.; Chang, W.; Nie, J. *Progr. Org. Coat.* **2013**, *76*, 471.



29. Bayramoglu, G.; Kahraman, M. V.; Kayaman-Apohan, N.; Gungor, A. *Progr. Org. Coat.* **2006**, *57*, 50.
30. Awaja, F.; Gilbert, M.; Kelly, G.; Fox, B.; Pigram, P. J. *Progr. Polym. Sci.* **2009**, *34*, 948.
31. Qin, X.; Xiong, J.; Yang, X.; Wang, X.; Zheng, Z. *J. Appl. Polym. Sci.* **2007**, *104*, 3554.
32. Kundakci, S.; Uezuem, O. B.; Karadag, E. *React. Funct. Polym.* **2008**, *68*, 458.
33. Xing, C. M.; Deng, J. P.; Yang, W. T. *Polym. J.* **2002**, *34*, 801.
34. Weikart, C. M.; Miyama, M.; Yasuda, H. K. *J. Colloid Interface Sci.* **1999**, *211*, 18.
35. Garg, M. S.; Srivastava, D. *Progr. Org. Coat.* **2014**, *77*, 1208.
36. Park, S. J.; Lee, S. G. *J. Colloid Interface Sci.* **2000**, *228*, 90.
37. Yan, Z.; Liu, W.; Gao, N.; Wang, H.; Su, K. *Appl. Surface Sci.* **2013**, *284*, 683.
38. Yilgor, E.; Yurtsever, E.; Yilgor, I. *Polymer* **2002**, *43*, 6561.
39. Diao, Yan, H.; Qiu, F.; Lu, L.; Lu, J.; Lin, X.; Li, B.; Shang, Q.; Liu, S.; Liu, W. *J. Macromolecules* **2010**, *43*, 6398.
40. Gurtekin, M.; Kayaman-Apohan, N.; Kahraman, M. V.; Menciloglu, Y.; Gungor, A. *React. Funct. Polym.* **2009**, *69*, 698.
41. Cui, J.; Yu, G.; Pan, C. *J. Appl. Polym. Sci.* **2014**, *131*, 131.
42. Abate, L.; Blanco, I.; Cicala, G.; Mamo, A.; Recca, G.; Scamporrino, A. *Polym. Degrad. Stabil.* **2010**, *95*, 798.